

Title page

Amino-pyrrolidine tricarboxylic acids (APTCs) give new insight into group III metabotropic glutamate receptor activation mechanism

Mélanie Frauli, Nadia Hubert, Stephan Schann, Nicolas Triballeau, Hugues-Olivier Bertrand, Francine Acher, Pascal Neuville, Jean-Philippe Pin, and Laurent Prézeau

Faust Pharmaceuticals SA, 67400 Illkirch-Graffenstaden, France (MF, NH, SS, PN).

Département de Pharmacologie Moléculaire, Institut de Génomique Fonctionnelle; CNRS UMR 5203, 34094 Montpellier, France ; INSERM U661, 34094 Montpellier, France ; Univ. Montpellier I, 34094 Montpellier, France ; Univ. Montpellier II, 34094 Montpellier, France (MF, JPP, LP).

Laboratoire de Chimie et Biochimie Pharmacologiques et Toxicologiques ; CNRS UMR 8601, Université René Descartes-Paris V, 75270 Paris Cedex 06, France (NT, FA).

Accelrys SA, 91893 Orsay Cedex, France (NT, HOB).

Running title page

Running title:

APTCs as tools to study group III mGlu receptor activation.

Corresponding author:

Laurent Prézeau

Institut de Génomique Fonctionnelle; 141, rue de la Cardonille; 34094 Montpellier, France

Telephone: 33 (0)4 67 14 29 33 - Fax: 33 (0)4 67 54 24 32

E-mail: laurent.prezeau@igf.cnrs.fr

| | |
|------------------------------------------|------|
| Number of text pages: | 30 |
| Number of tables: | 1 |
| Number of figures: | 6 |
| Number of references: | 42 |
| Number of words in <i>Abstract</i> : | 250 |
| Number of words in <i>Introduction</i> : | 737 |
| Number of words in <i>Discussion</i> : | 1285 |

Non-standard abbreviations:

VFT: Venus Fly-trap; APTCs: amino-pyrrolidine tricarboxylic acids; GPCRs: G-protein coupled receptors; LBD: ligand binding domain; iGlu: ionotropic glutamate receptor; mGlu: metabotropic glutamate receptor;

Abstract

Like most class-C G-protein coupled receptors, metabotropic glutamate (mGlu) receptors possess a large extracellular domain where orthosteric ligands bind. Crystal structures revealed that this domain, called Venus Fly-trap (VFT), adopts a closed vs. open conformation upon agonist or antagonist binding, respectively. Recently, we described aminopyrrolidine tricarboxylic acids (APTCs), including FP0429, as new selective group III mGlu agonists. Whereas FP0429 is an almost full mGlu4 agonist, it is a weak and partial agonist of the closely-related mGlu8 subtype. To get more insight into the activation mechanism of mGlu receptors, we aimed at elucidating why FP0429 behaves differently at these two highly homologous receptors, by focusing on two residues within the binding site that differ between mGlu4 and mGlu8. Site-directed mutagenesis of S157 and G158 of mGlu4 into their mGlu8 homologues (Ala) turned FP0429 into a weak partial agonist. Conversely, introduction of Ser and Gly residues into mGlu8 increased FP0429 efficacy. Docking of FP0429 in mGlu4 VFT 3D model helped us characterize the role of each residue. Indeed, mGlu4 S157 seems to have an important role in FP0429 binding, while G158 may allow a deeper positioning of this agonist in the cavity of lobe I, thereby ensuring optimal interactions with lobe-II residues in the fully closed state of the VFT. In contrast, the presence of a methyl group in mGlu8 (Ala instead of Gly) weakens the interactions with the lobe-II residues. This probably results in a less stable or a partially closed form of the mGlu8 VFT, leading to partial receptor activation.

Introduction

In the brain, glutamate (Glu) is the transmitter of most fast excitatory synapses, acting on either ionotropic glutamate (iGlu) or metabotropic glutamate (mGlu) receptors, which belong to the class-C of G-protein coupled receptors (GPCRs). The ligand binding domain (LBD) of mGlu receptors was shown to adopt a so-called Venus FlyTrap (VFT) fold, composed of two lobes interconnected by a flexible hinge (Kunishima et al., 2000). Agonists bind to lobe I, and are then trapped in the cleft upon VFT closure, while competitive antagonists keep the VFT domain in an open conformation (Bessis et al., 2002; Tsuchiya et al., 2002). Crystal structures (Kunishima et al., 2000; Tsuchiya et al., 2002) and homology models (Bertrand et al., 2002; Bessis et al., 2000; Malherbe et al., 2001; Rosemond et al., 2004) of both open and closed conformations of the VFT domain have been reported for most of the eight cloned mGlu receptor subtypes.

According to their sequence similarity and transduction mechanism, but also their pharmacology, the eight mGlu receptors have been further classified into three groups (Pin and Acher, 2002). Group III mGlu receptors, i.e. mGlu4, 6, 7 and 8 subtypes, are coupled to *Pertussis* toxin-sensitive Gi and/or Go G-proteins and are activated by group-specific agonists like L-AP4 or ACPT-I (Acher et al., 1997; Nakanishi, 1992). While mGlu6 receptor expression is restricted to the bipolar cells of the retina, subtypes mGlu4, 7 and 8 are expressed throughout the brain on nerve terminals, preferentially on the presynaptic region, where they exert a control on neurotransmitter release (Schoepp, 2001). Localization studies have shown that subtype mGlu7 is located directly in the synaptic cleft, while mGlu4 and 8 are mostly present at perisynaptic sites outside the active zone of neurotransmitter release. These diverse localizations may indicate separate roles in regulating Glu release and spill-over effects, and may also account for the fact that the affinities of group III mGlu receptors for their natural ligand Glu, and many other well characterized agonists, vary over a very

large concentration range (Schoepp et al., 1999). The molecular basis for these affinity discrepancies was recently investigated: residues of the LBD, but also additional residues of the N-terminus, were identified as determinants of the pharmacological profile of group III receptors (Rosemond et al., 2004). Interestingly, out of the dozen of residues usually considered as constituting the LBD of mGlu receptors, only two differ between mGlu4 and mGlu8 subtypes. Therefore, very few agonists have been described to have significantly different pharmacological properties on these two receptor subtypes (De Colle et al., 2000). One of the only exceptions is S-3,4-DCPG, showing nanomolar potency toward subtype mGlu8, and only low micromolar potency for mGlu4 (Thomas et al., 2001).

We recently described a new family of molecules, the amino-pyrrolidine tricarboxylic acids (APTCs), whose design was based on medicinal chemistry around group III specific agonist ACPT-I (Acher et al., 1997). The APTC head of series, FP0429, presented the very attractive feature of behaving as an almost full agonist on mGlu4, while being a very weak partial agonist on mGlu8 (Schann et al., 2006). This FP0429 compound therefore appeared as an exciting tool to decipher partial agonism mechanism regarding mGlu receptors. Indeed, concerning partial agonists, no specific studies have yet been reported with class-C GPCRs. However, suggestions to explain the mode of action of several partial agonists of receptors holding a similar VFT domain, i.e. the iGlu receptors, have been made and recently reviewed (Chen and Wyllie, 2006; Mayer, 2005). Efficacy of activation of these receptors was correlated to either the extent of VFT closure or to the stabilization degree of the VFT closed state.

In the present study, we performed site-directed mutagenesis on the residues differing between mGlu4 and mGlu8 LBD (i.e. S157 and G158 in mGlu4, which respectively align with A154 and A155 in mGlu8) and analyzed the functional responses of the mutant receptors to both Glu and FP0429, by measuring intracellular Ca^{2+} mobilization. We also docked

FP0429 in the previously described 3D model of mGlu4 LBD (Bertrand et al., 2002) to draw hypotheses explaining the impact of the presence of different residues in either mGlu4 or mGlu8 on FP0429 binding and subsequent VFT closure. Collectively, information derived from both mutagenesis study and 3D models converged to demonstrate the importance of A154 and A155 in preventing FP0429 to fully activate mGlu8, thereby giving insight into mGlu partial agonist activation mechanism by either partial VFT closure or weaker stabilization of the closed VFT domain.

Materials and Methods

Materials

FP0429 was synthesized as described previously (Schann et al., 2006). Glutamate and ACPT-I (1-aminocyclopentane 1,3,4-tricarboxylic acid) were purchased from Sigma-Aldrich (Lyon, France) and Tocris Cookson (Bristol, U.K.), respectively.

Culture medium, Fetal Calf Serum (FCS), and all other products used for cell culture were purchased from PAA laboratories (Les Mureaux, France). Fluo4-AM was purchased from Molecular Probes (Leiden, The Netherlands).

All reagents for the ELISA assay (Para formaldehyde, Triton TX100, Bovine Serum Albumin and Tween20) were purchased from Sigma-Aldrich (Lyon, France). Anti-HA mouse 4C12 monoclonal antibody was purchased from Abcam (Cambridge, U.K.). HRP-conjugated goat anti-mouse secondary antibody and revelation kit Amplex Red ELISA II were purchased from Invitrogen (Cergy Pontoise, France).

Cell Culture and Transfection

HEK293 cells were cultured in modified Eagle's medium (MEM) supplemented with 10% FCS and transfected by electroporation as previously described (Brabet et al., 1998; Frauli et al., 2006). For intracellular Ca^{2+} measurement and ELISA assay, 5 million cells were transfected with 5 μg plasmid DNA encoding rat mGlu4 or mGlu8 receptors (either wild-type or mutants). The construction of the plasmids expressing wild-type mGlu receptors has been described previously (Gomez et al., 1996; Joly et al., 1995; Parmentier et al., 1998). Receptors were coupled to the Phospholipase C pathway by co-transfection with 2 μg of plasmid DNA encoding the chimeric $\text{G}_{\text{q}19}$ protein (Gomez et al., 1996). For partial/full agonism experiments, 3 million cells were transfected with increasing amounts of mGlu-

encoding plasmid DNA, ranking from 0 (Mock) to 5 μ g, completed to a total amount of 5 μ g DNA with carrier vector pRK6.

Site-directed mutagenesis

Mutagenesis was performed using the Gene Tailor Site Directed Mutagenesis system from Invitrogen. Polymerase Chain Reactions were performed using the high fidelity Pfu DNA Polymerase (Promega, Charbonnières, France) and specific forward primers (MWG Biotech, Ebersberg, Germany) for the different constructions: mGlu4SA (i.e. with S157 and G158 mutated in SA; tgggtgtcattggagcttcagcgagctccgtctcg), mGlu4AG (mutation of SG in AG; agtgggtgggtgtcattggagctgcagggagctccgtctc), mGlu4AA (mutation of SG in AA; tgggggtgtcattggagctgcagcgagctccgtctcg), mGlu8SA (i.e. with A154 and A155 mutated in SA; tttctggcgtcataggtgcttcagcaagctctgtg), mGlu8AG (mutation of AA in AG; ctggcgtcataggtgctgcaggaagctctgtgtcc), and mGlu8SG (mutation of AA in SG; tttctggcgtcataggtgcttcaggaagctctgtgtcc). For the 3 mutant constructions of each mGlu receptor, a single reverse primer was used (mGlu4: agtccaatgacaccaccactcgttcggg; mGlu8: agcacctatgacgccagaaatcttgtcggg).

Intracellular Calcium Measurements

After transfection, cells were seeded in polyornithine-coated, black-walled, clear bottom 96-well plates and cultured for 24 h. Cells were washed with freshly prepared buffer (1x HBSS supplemented with 20 mM HEPES, 1 mM MgSO₄, 3.3 mM Na₂CO₃, 1.3 mM CaCl₂, 2.5 mM Probenecid and 0.5 % BSA) and loaded with 1 μ M Ca²⁺-sensitive fluorescent dye Fluo-4 AM for 1h30min at 37°C. After washing, cells were incubated with 50 μ l of buffer; 50 μ l of 2x-drug solution (prepared in buffer) was then added by the fluorescence microplate reader FlexStation II384 (Molecular Devices, Sunnyvale, CA, USA) in each well after 20 s of

recording. Fluorescence signals (excitation 485 nm, emission 525 nm) were then measured at sampling intervals of 1.5 s for 60 s.

ELISA assay

The procedure of the ELISA assay on intact cells was described previously (Goudet et al., 2004). Briefly, after 24h of culture in polyornithine-coated, black-walled, clear bottom 96-well plates, electroporated cells were fixed with PBS 4% Para-formaldehyde, then half of the wells were permeabilized using PBS 0.05% Triton TX100. Blocking of unspecific binding sites and cell incubations with antibodies (1:1000 dilutions of either primary anti-HA 4C12 or secondary HRP-conjugated anti-mouse antibody) were performed in PBS 1% Bovine Serum Albumin. Washing steps after antibody incubations were performed using PBS 0.05% Tween20. Revelation was performed using the Amplex Red ELISA II kit, according to manufacturer's instructions.

Sequence alignment

For group III mGlu sequence alignment, the following SwissProt or GenBank accession numbers were used: P31423 (rat mGlu4), NM_001013385.1 (mouse mGlu4), Q14833 (human mGlu4), P70579 (rat mGlu8), P47743 (mouse mGlu8), and O00222 (human mGlu8). Full length sequence alignment was performed using the ClustalW multiple alignment program (Thompson et al., 1994) at http://www.infobiogen.fr/services/analyseseq/cgi-bin/clustalw_in.pl.

3D modelling of mGlu extracellular domains, ligand docking and complex refinement in the model

Homology modelling of mGlu receptor LBD and molecular docking were performed according to the protocol described by Bessis *et al.* and Bertrand *et al.* (Bertrand et al., 2002;

Bessis et al., 2000). Comparative models were generated using MODELER 7.00 based on the coordinates of mGlu1 receptor LBD (PDB Code: 1ewk) (Kunishima et al., 2000). Our previously validated docking protocol (Triballeau et al., 2005), consisted first in the flexible fitting of the ligand within the rigid receptor using the shape-based docking algorithm LigandFit (Venkatachalam et al., 2003). The obtained poses were subsequently scored using the LigScore2 scoring function (Krammer et al., 2005). The best pose was then energy minimized with CHARMM (Brooks et al., 1983) allowing full flexibility for both ligand and receptor. Solvation effects were explicitly taken into account by embedding the binding cleft in a 25 Å sphere of water molecules (model TIP3P). The sphere of water was centred on the geometric centre of the ligand and restrained using an MMFP potential. All calculations were carried out in the Discovery Studio 1.5 environment (Accelrys Inc., San Diego, 92121 CA).

Data analysis

The dose-response or partial/full agonism curves were fitted using the GraphPad (San Diego, CA, USA) PRISM program. All data are mean \pm sem from at least 3 individual experiments performed in triplicates. ANOVA analysis of independent experiments was performed with a general linear model using a Dunnett test (MiniTab14 for Windows, Minitab Inc., Pennsylvania, USA).

Results

Effects of FP0429 on wild-type group III mGlu receptors

Amino-pyrrolidine tricarboxylic acids (APTCs) were designed on the basis of structural modifications of 1-amino-cyclopentane 1,3,4-tricarboxylic acid (ACPT-I), in order to obtain a scaffold close to ACPT-I with similar highly polar side chains, and amenable to parallel synthesis. A virtual library of one hundred APTCs was designed, 65 compounds were finally synthesized, and then tested on all mGlu subtypes (Schann et al., 2006). FP0429 (Figure 1A) was found to be highly interesting, as it did not interact with either group I or II mGlu receptors at up to 5mM, while showing agonist activity at group III mGlu receptors.

FP0429 dose-response curves were performed on cells transfected with wild-type (wt) mGlu4 or mGlu8, in comparison with Glu (Figure 1B and C, respectively). FP0429 EC₅₀ values were comparable for both receptors (48.3±5.2 and 56.2±14.6 μM, respectively; Table 1) while a clear difference could be observed in the E_{max} values, with respect to the Glu maximal effect. Indeed, FP0429 dose-response amplitude on wt mGlu4 was comparable to that of Glu (Figure 1B), while the compound gave partial responses on wt mGlu8 (Figure 1C), corresponding only to 36±7% of the Glu maximum, under these conditions (Table 1).

As this difference in response amplitude could be explained by partial agonism of FP0429 on wt mGlu8, this issue was further examined, by testing the effects of maximal doses of Glu, FP0429 or ACPT-I on cells transfected with increasing amounts of receptor plasmid DNA. As shown in Figure 2A, ACPT-I maximal effect on mGlu4 was similar to that generated by Glu whatever the expression level of cell surface receptor, as quantified using ELISA assay on intact cells. This demonstrates that ACPT-I is definitely a full agonist at this receptor subtype. It is noteworthy that the maximal effect of FP0429 was always somewhat lower than that obtained with Glu (with values comprised between 70 and 95%), suggesting that this compound is a partial agonist with high efficacy regarding mGlu4 (and as such we decided to

call it an “almost full agonist”) (Figure 2A). On the contrary, when a similar experiment was performed on cells expressing various amounts of mGlu8, the maximal effect of FP0429 was always dramatically weaker than that of Glu (Figure 2B). Indeed, at low receptor expression level, when the presence of reserve receptor is very unlikely, the maximal effect of FP0429 reached only 6 to 10% of that of Glu, demonstrating that this compound is a very weak partial agonist on this receptor subtype (Figure 2B). Besides, these data as well indicate that ACPT-I is a partial agonist on mGlu8, generating responses equal to 37 to 41% of that of Glu at low receptor expression level (Figure 2B).

The partial agonist activity of FP0429 at mGlu8 was further characterized by testing its bivalent agonist and antagonist activity (Figure 2C). Indeed, in the presence of a sub-maximal Glu dose (here, 5 μ M), FP0429 behaved as an antagonist, decreasing Glu response down to its own maximum and not to basal level (as a full antagonist would have done). Using the equation $K_B = IC_{50}/(1+L/EC_{50})$, where L is the Glu concentration in the experiment, and EC₅₀ the mean experimental Glu EC₅₀ at mGlu8 (see Table 1), the K_B value obtained in these experimental conditions (74.6 μ M) was, as expected, close to FP0429 EC₅₀ value for mGlu8 (56.2 \pm 14.6 μ M; Table 1).

Potential molecular determinants involved in FP0429 full or partial agonism on group III mGlu receptors

Information on the potential molecular determinants involved in this differential agonist activity came from ACPT-I docking in wt mGlu4 ligand binding pocket 3D model (Bertrand et al., 2002; Bessis et al., 2000) (Figure 3A). In this model, 15 amino-acid residues from both lobe I and lobe II are involved in ligand binding or surrounding it. Alignments of mouse, rat and human mGlu4 and 8 sequences demonstrated the perfect conservation of 13 residues among each receptor subtype in these three mammalian species, but revealed that 2 residues

differed between these two receptor subtypes (Figure 3B). Indeed, mGlu4 S157 and G158 align with 2 Ala residues in the three mammalian mGlu8 sequences (A154 and 155) (Figure 3B). Moreover, a homology model of the mGlu4 binding site docked with FP0429 showed a close contact between G158 and the fumaryl side chain of FP0429 (see below). We therefore decided to investigate the potential role of these 2 residues in the differential activity of FP0429 at mGlu4 and mGlu8.

Expression and function of the mutated mGlu4 and mGlu8 receptors

For each of the 2 residues potentially involved in FP0429 differential agonist efficacy on subtypes mGlu4 and mGlu8, we constructed mutant receptors bearing either a single (mGlu4SA, mGlu4AG, mGlu8SA and mGlu8AG) or a double mutation (mGlu4AA (“mGlu8-like”) and mGlu8SG (“mGlu4-like”)). As all wt and mutant receptors were tagged with an HA-epitope, their expression was checked using anti-HA ELISA assay. All mGlu4 and mGlu8 mutants were expressed at the same level as their wt counterparts at the cell surface of transfected HEK293 cells (Figures 4A and C for mGlu4 and mGlu8 wt and mutant receptors, respectively). In agreement with this observation, Glu generated similar Ca^{2+} signals to those produced by wt receptors (Figures 4B and D for mGlu4 and mGlu8 wt and mutant receptors, respectively).

Impact of the mutations on receptor responses to FP0429

The fact that the mGlu4 and mGlu8 mutant receptors responded to their natural ligand Glu as efficiently as wt receptors was confirmed by dose-response experiments (Figures 5A and 5B). Indeed, these dose-dependence curves were identical for both wt and mutated receptors, regarding both signal amplitude (E_{max}) and EC_{50} (Table 1; for mGlu4, compare Figure 5A and 1B; for mGlu8, compare Figure 5B and 1C).

Interestingly, if Glu responses were not modified after introduction of the mutations, on the contrary, receptor challenged with FP0429 gave, as predicted, different responses. Concerning mGlu4, the SG into SA mutation had no real effect on the EC50 value (40.1 ± 3.8 vs. $48.3 \pm 5.2 \mu\text{M}$; no statistically significant difference), but significantly impacted on the Emax value, which was decreased 1.5 fold, indicating the importance of the G158 residue (Figure 5A; Table 1). The double mutant mGlu4AA displayed not only this decreased Emax value, but also a lower affinity for FP0429, as its EC50 was significantly increased 1.6 fold ($79.6 \pm 14.3 \mu\text{M}$ vs. $48.3 \pm 5.2 \mu\text{M}$; $p < 0.01$; Figure 5A; Table 1), demonstrating the importance of the S157 residue, although the single mutant of this specific residue (mGlu4AG) was found to behave like the wt receptor, concerning both EC50 and Emax values.

Mutant mGlu8 receptors did not differ much from wt receptor as far as FP0429 EC50 was concerned (Figure 5B; Table 1). As observed for mGlu4, the real impact of the point mutations concerned the Emax value, which was found to be strongly increased, respectively 1.4-, 1.9- and 2.5-fold for mGlu8SA, mGlu8AG and mGlu8SG. The resulting Emax values, as expressed in % Glu max, reached 52 ± 8 , 70 ± 11 and $90 \pm 16\%$, for mGlu8SA, mGlu8AG and mGlu8SG, respectively, to be compared with $36 \pm 7\%$ for wt mGlu8 at the same receptor expression level (Table 1).

Further experiments were performed with the “mGlu4-like” mGlu8SG receptor; as described for Figure 2B, a maximal dose of Glu, ACPT-I or FP0429 was applied on cells transfected with increasing amounts of mGlu8SG plasmid DNA (Figure 5C). It is noteworthy that both FP0429 and ACPT-I curves were shifted upwards, and were now almost comparable to the Glu curve. At low cell surface receptor level, the signal values, as expressed in percentage of the Glu maximal response, reached at least 60% for FP0429, and from 75 to 90% for ACPT-I, to be compared with 6 to 10%, and 37 to 41% with wt mGlu8, respectively (Figure 2B). This

demonstrates that the two residues AA in mGlu8 are responsible for the partial agonist activity of both ACPT-I and FP0429.

3D docking of FP0429 in mGlu4 ligand binding site

Dockings at mGlu4 binding site revealed that most of the binding features observed for ACPT-I (Bertrand et al., 2002; Bessis et al., 2000) are conserved for its close analog FP0429 (compare Figures 3A and 6A). The α -amino acid function of both ligands binds similarly to a set of conserved proximal residues that build up a signature motif as previously described (Acher and Bertrand, 2005; Bertrand et al., 2002). The polar distal functions of ACPT-I (3- and 4-CO₂H) and of FP0429 (2-CO₂H, CO of amide, fumarate) interact with the same set of distal residues from the two lobes (except for S110). However, the distribution of the hydrogen bonds and ionic interactions appears somewhat different between the two ligands, and may explain the difference in potencies between ACPT-I and FP0429 at mGlu4. Interestingly, FP0429 is trapped in this dense network of polar bonds in a specific conformation with no possible flexibility. Thus, the β -ethylenic proton of FP0429 is brought in close vicinity (2.1 Å) of the α -proton of G158 (see arrow in Figure 6A). When this G158 proton is replaced by the methyl group of an Ala residue, a steric hindrance would be observed if the polar network was kept as in wt mGlu4. Consequently, to avoid the steric clash with A155 of mGlu8, a shift of FP0429 is observed (compare Figures 6C (mGlu4) and 6D (mGlu8); Figure 6E) in the homology model of the mGlu8 closed conformation. This shift in the positioning of FP0429 induces a modification of the polar distal bindings (Figure 6B), while maintaining the proximal binding as in mGlu4. In this mGlu8 model, we assume that the same extent of domain closure is reached as with mGlu4 full agonists. A close inspection of this model reveals that on one hand, binding of FP0429 to lobe I is roughly similar to that of FP0429 bound to mGlu4, and that on the other hand, some polar bindings to lobe II are

missing (N283 and R255 in mGlu8) (Figures 6B and D). Moreover, it also shows that less inter-lobe interactions are present in the mGlu8 model compared to the mGlu4 model docked with FP0429 (not shown in Figures). Altogether, the comparison of the two models attests of a weaker stability of the closed liganded form of the mGlu8 VFT.

Discussion

The amino-pyrrolidine tricarboxylic acid (APTC) FP0429 was recently described as a specific group III mGlu receptor agonist (Schann et al., 2006). In the present study, we demonstrate the partial agonist activity of FP0429 on mGlu8. Although it displayed a similar potency at both mGlu4 and mGlu8 receptors, FP0429 has a much lower efficacy at the latter subtype vs its related homolog mGlu4. Indeed, FP0429 efficacy at mGlu8 represents only 6-10% of that of the full agonist Glu, at low receptor expression level. We identified the two residues of the ligand binding pocket that differ between mGlu8 and mGlu4, and which are responsible for FP0429 differential efficacy. Finally, 3D modeling and docking experiments provided putative explanation for FP0429 partial agonism towards mGlu8 receptor.

The partial agonist activity of FP0429 at mGlu8 was suggested in our previous study by its maximal effect reaching only 36% of that of Glu at high receptor expression (Schann et al., 2006). Here we confirmed this observation and further demonstrated the partial agonist character of FP0429 by showing that FP0429 was equally potent at activating mGlu8 and at inhibiting the sub-maximal effect of Glu on this receptor. However, the measured efficacy of a partial agonist depends first on its real agonist efficacy, but also on the presence of receptor reserve. Thus, in the presence of a large amount of receptor reserve, a partial agonist can still reach the maximal limit of the response, and therefore can behave as a full agonist. As such, to determine the real efficacy of FP0429 at both mGlu4 and mGlu8, its maximal effect was compared to that of Glu at various receptor surface expression levels. Thus, the minimal efficacy of FP0429 is 6-10% of that of glutamate on mGlu8, whereas it is more than 70% on mGlu4. Actually, due to the strong binding site conservation between wt mGlu4 and 8, most group III ligands described so far usually present comparable activity on both subtypes. This is the case for Glu, linear Glu analogs like L-SOP, L-AP4 or MAP-4, cyclopropyl analogs like DCG-IV or phenylglycines like 3,5-DHPG, MPPG or PPG (De Colle et al., 2000; Pin and

Acher, 2002). Today, only few ligands may discriminate between group -III mGluRs, like the phenylglycine S-3,4-DCPG that is 10-100 times more potent at mGlu8 than mGlu4 (Thomas et al., 2001), or the positive allosteric modulators PHCCC, AMN082 and mGluR8-B that are selective for mGlu4 (Maj et al., 2003), mGlu7 (Mitsukawa et al., 2005) and mGlu8 (Wilson et al., 2005), respectively. Thus, by almost fully activating mGlu4 and inhibiting sub-maximal effects of Glu at mGlu8, FP0429 is a good tool to discriminate between these subtypes of group-III mGluRs in the brain.

A number of recent studies examined the molecular events leading to partial agonist activity at class-A GPCRs. These studies are consistent with partial agonists stabilizing a specific conformation of the receptor (Baneres et al., 2005; Ghanouni et al., 2001; Kim et al., 2006; Nikolaev et al., 2006), being able to unlock some but not all the locks that maintain the receptor in its inactive state (Seifert et al., 2001). However, the activation mechanism of class-C GPCRs appears more complex, with the agonist binding site being located in the VFT, within the large extracellular domain. The high sequence identity between mGlu4 and mGlu8, and the difference of FP0429 efficacy at these two receptors, offer a nice opportunity to identify the molecular determinants responsible for partial activity at class-C GPCRs.

We found that two residues that differ between mGlu4 and mGlu8 binding sites are responsible for the differential efficacy of FP0429 at these two receptors. Indeed, replacement of S157 and G158 of mGlu4 by the mGlu8 residues (Ala in both cases) converted FP0429 into a partial agonist. Conversely, replacement of A154 and A155 by S and G in mGlu8 largely increased FP0429 efficacy. Single point mutations also revealed a major role of the G158 (mGlu4) and A155 (mGlu8), in this phenomenon. Interestingly, all mutants of both mGlu4 and mGlu8 responded to glutamate stimulation exactly like their wt counterparts. This was in agreement with the effect of linear glutamate analogs on S157 or G158 mutated mGlu4 or mGlu8 receptors (Hampson et al., 1999; Rosemond et al., 2002). Thus, even with the

introduction of more “bulky” residues (mutation of G158 into Ala) in the LBD, the flexibility of Glu (or other linear ligands), which can adopt many conformations, and the potential presence in the pocket of “buffering” water molecules, could explain the absence of impact of the different mutations on Glu-induced functional responses.

To further examine the role of the identified residues in the agonist efficacy of FP0429, docking experiments were conducted in closed form 3D models of mGlu4 and mGlu8 VFTs. FP0429 partial agonist activity on mGlu8 seems to involve residues located away from the hinge and interacting with the distal functions of the ligand, or involved in inter-lobe contacts. On the mGlu4 model depicted in Figure 6A, the H atom from G158 is in close vicinity (2.1 Å) of the ethylenic H atom from FP0429. We hypothesized that the presence of a bulkier residue in mGlu8 (Ala vs. Gly) could induce a steric hindrance forcing FP0429 to position itself differently at lobe I, creating a shift in the molecule position in mGlu8 vs. mGlu4. This results in a different orientation of the side chain of FP0429, and a different position of the side chain of several residues both from lobe I and lobe II. As a consequence, fewer inter-domain interactions could be formed, likely resulting in a weaker stabilization of the closed state of the mGlu8 VFT, explaining the low agonist efficacy of this compound at mGlu8. Although AMPA and NMDA receptors are ligand-gated channels, their agonist binding site also consists of a VFT domain. Of interest, the 3D crystal structure of the VFT domain of the NMDA receptor NR1 subunit has been solved with either the full agonist glycine or various partial agonists with increasing size (Inanobe et al., 2005). In all cases, a fully closed state was observed. As proposed here for FP0429 at mGlu8, the partial agonist activity at the NR1 subunit was therefore explained by a lower stabilization of the closed state of the VFT, resulting in that case from an incomplete change in conformation of the second VFT inter-domain (Inanobe et al., 2005).

However, our docking experiments were performed in a model of the closed conformation of the mGlu8 VFT. Indeed, only a fully closed and a widely open conformation of the mGlu1 VFT are available as templates, thus it was not possible to dock FP0429 in a partially closed state of the mGlu8 VFT. As such, we cannot exclude the possibility that a different interacting mode of FP0429 in the lobe I of the open form of mGlu8 may generate a hindrance preventing the full closure of the VFT. Such a partially closed state may then be responsible for the low agonist efficacy. This second proposal is consistent with structural data obtained with the GluR2 subunit, since kainate, a partial AMPA receptor agonist, stabilizes the GluR2 VFT in a partially closed form (Armstrong et al., 2003), and that the extent of domain closure is related to the agonist efficacy (Jin et al., 2003). Whether this is also the case for mGlu receptor remains to be further studied.

To conclude on the present work, using a newly described group III mGlu agonist, and combined approaches of both site-directed mutagenesis and 3D modelling, we propose a dual mechanism for mGlu receptor partial agonism. The two hypotheses that are envisaged are not mutually exclusive, and consist, upon partial agonist binding, in either a partially closed form of the VFT domain or a less stable fully closed conformation of this domain.

Acknowledgements

The authors wish to thank Dr Stanislas Mayer and Géraldine Mercier for their help in the laboratory.

Reference List

- Acher FC and Bertrand HO (2005) Amino acid recognition by Venus flytrap domains is encoded in an 8-residue motif. *Biopolymers* **80**:357-66.
- Acher FC, Tellier FJ, Azerad R, Brabet IN, Fagni L and Pin JP (1997) Synthesis and pharmacological characterization of aminocyclopentanetricarboxylic acids: new tools to discriminate between metabotropic glutamate receptor subtypes. *J Med Chem* **40**:3119-3129.
- Armstrong N, Mayer M and Gouaux E (2003) Tuning activation of the AMPA-sensitive GluR2 ion channel by genetic adjustment of agonist-induced conformational changes. *Proc Natl Acad Sci U S A* **100**:5736-5741.
- Baneres JL, Mesnier D, Martin A, Joubert L, Dumuis A and Bockaert J (2005) Molecular characterization of a purified 5-HT₄ receptor: a structural basis for drug efficacy. *J Biol Chem* **280**:20253-20260.
- Bertrand HO, Bessis AS, Pin JP and Acher FC (2002) Common and selective molecular determinants involved in metabotropic glutamate receptor agonist activity. *J Med Chem* **45**:3171-3183.
- Bessis AS, Bertrand HO, Galvez T, De Colle C, Pin JP and Acher F (2000) Three-dimensional model of the extracellular domain of the type 4a metabotropic glutamate receptor: new insights into the activation process. *Protein Sci* **9**:2200-2209.
- Bessis AS, Rondard P, Gaven F, Brabet I, Triballeau N, Prezeau L, Acher F and Pin JP (2002) Closure of the Venus flytrap module of mGlu8 receptor and the activation process: Insights from mutations converting antagonists into agonists. *Proc Natl Acad Sci U S A* **99**:11097-11102.
- Brabet I, Parmentier ML, De Colle C, Bockaert J, Acher F and Pin JP (1998) Comparative effect of L-CCG-I, DCG-IV and gamma-carboxy-L-glutamate on all cloned metabotropic glutamate receptor subtypes. *Neuropharmacology* **37**:1043-1051.
- Brooks BR, Bruccoleri RE, Olafson BD, States DJ, Swaminathan S and Karplus M (1983) CHARMM: A Program for Macromolecular Energy, Minimization, and Dynamics Calculations. *J Comp Chem*:187-217.
- Chen PE and Wyllie DJ (2006) Pharmacological insights obtained from structure-function studies of ionotropic glutamate receptors. *Br J Pharmacol* **147**:839-853.
- De Colle C, Bessis AS, Bockaert J, Acher F and Pin JP (2000) Pharmacological characterization of the rat metabotropic glutamate receptor type 8a revealed strong similarities and slight differences with the type 4a receptor. *Eur J Pharmacol* **394**:17-26.
- Frauli M, Neuville P, Vol C, Pin JP and Prezeau L (2006) Among the twenty classical L-amino acids, only glutamate directly activates metabotropic glutamate receptors. *Neuropharmacology* **50**:245-253.
- Ghanouni P, Gryczynski Z, Steenhuis JJ, Lee TW, Farrens DL, Lakowicz JR and Kobilka BK (2001) Functionally different agonists induce distinct conformations in the G protein coupling domain of the beta 2 adrenergic receptor. *J Biol Chem* **276**:24433-24436.
- Gomez J, Mary S, Brabet I, Parmentier ML, Restituito S, Bockaert J and Pin JP (1996) Coupling of metabotropic glutamate receptors 2 and 4 to G alpha 15, G alpha 16, and chimeric G alpha q/i proteins: characterization of new antagonists. *Mol Pharmacol* **50**:923-930.

- Goudet C, Gaven F, Kniazeff J, Vol C, Liu J, Cohen-Gonsaud M, Acher F, Prezeau L and Pin JP (2004) Heptahelical domain of metabotropic glutamate receptor 5 behaves like rhodopsin-like receptors. *Proc Natl Acad Sci U S A* **101**:378-383.
- Hampson DR, Huang XP, Pekhletski R, Peltekova V, Hornby G, Thomsen C and Thogersen H (1999) Probing the ligand-binding domain of the mGluR4 subtype of metabotropic glutamate receptor. *J Biol Chem* **274**:33488-33495.
- Inanobe A, Furukawa H and Gouaux E (2005) Mechanism of partial agonist action at the NR1 subunit of NMDA receptors. *Neuron* **47**:71-84.
- Jin R, Banke TG, Mayer ML, Traynelis SF and Gouaux E (2003) Structural basis for partial agonist action at ionotropic glutamate receptors. *Nat Neurosci* **6**:803-810.
- Joly C, Gomeza J, Brabet I, Curry K, Bockaert J and Pin J-P (1995) Molecular, functional and pharmacological characterization of the metabotropic glutamate receptor type 5 splice variants: comparison with mGluR1. *J. Neurosci.* **15**:3970-3981.
- Kim SK, Gao ZG, Jeong LS and Jacobson KA (2006) Docking studies of agonists and antagonists suggest an activation pathway of the A(3) adenosine receptor. *J Mol Graph Mode* **25**:562-577.
- Krammer A, Kirchhoff PD, Jiang X, Venkatachalam CM and Waldman M (2005) LigScore: a novel scoring function for predicting binding affinities. *J Mol Graph Model* **23**:395-407.
- Kunishima N, Shimada Y, Tsuji Y, Sato T, Yamamoto M, Kumasaka T, Nakanishi S, Jingami H and Morikawa K (2000) Structural basis of glutamate recognition by a dimeric metabotropic glutamate receptor. *Nature* **407**:971-977.
- Maj M, Bruno V, Dragic Z, Yamamoto R, Battaglia G, Inderbitzin W, Stoehr N, Stein T, Gasparini F, Vranesic I, Kuhn R, Nicoletti F and Flor PJ (2003) (-)-PHCCC, a positive allosteric modulator of mGluR4: characterization, mechanism of action, and neuroprotection. *Neuropharmacology* **45**:895-906.
- Malherbe P, Knoflach F, Broger C, Ohresser S, Kratzeisen C, Adam G, Stadler H, Kemp JA and Mutel V (2001) Identification of essential residues involved in the glutamate binding pocket of the group II metabotropic glutamate receptor. *Mol Pharmacol* **60**:944-954.
- Mayer ML (2005) Glutamate receptor ion channels. *Curr Opin Neurobiol* **15**:282-288.
- Mitsukawa K, Yamamoto R, Ofner S, Nozulak J, Pescott O, Lukic S, Stoehr N, Mombereau C, Kuhn R, McAllister KH, van der Putten H, Cryan JF and Flor PJ (2005) A selective metabotropic glutamate receptor 7 agonist: activation of receptor signaling via an allosteric site modulates stress parameters in vivo. *Proc Natl Acad Sci U S A* **102**:18712-18717.
- Nakanishi S (1992) Molecular diversity of glutamate receptors and implications for brain function. *Science* **258**:597-603.
- Nikolaev VO, Hoffmann C, Bunemann M, Lohse MJ and Vilardaga JP (2006) Molecular basis of partial agonism at the neurotransmitter alpha 2A-adrenergic receptor and Gi-protein heterotrimer. *J Biol Chem.* **281**:24506-24511.
- Parmentier ML, Joly C, Restituito S, Bockaert J, Grau Y and Pin JP (1998) The G protein-coupling profile of metabotropic glutamate receptors, as determined with exogenous G proteins, is independent of their ligand recognition domain. *Mol Pharmacol* **53**:778-786.
- Pin JP and Acher F (2002) The metabotropic glutamate receptors: structure, activation mechanism and pharmacology. *Curr Drug Targets CNS Neurol Disord* **1**:297-317.
- Rosemond E, Peltekova V, Naples M, Thogersen H and Hampson DR (2002) Molecular determinants of high affinity binding to group III metabotropic glutamate receptors. *J Biol Chem* **277**:7333-7340.

- Rosemond E, Wang M, Yao Y, Storjohann L, Stormann T, Johnson EC and Hampson DR (2004) Molecular basis for the differential agonist affinities of group III metabotropic glutamate receptors. *Mol Pharmacol* **66**:834-842.
- Schann S, Menet C, Arvault P, Mercier G, Frauli M, Mayer S, Hubert N, Triballeau N, Bertrand HO, Acher F and Neuville P (2006) Design and synthesis of APTCs (aminopyrrolidinetri-carboxylic acids): Identification of a new group III metabotropic glutamate receptor selective agonist. *Bioorg Med Chem Lett*. **16**:4856-4860.
- Schoepp DD (2001) Unveiling the functions of presynaptic metabotropic glutamate receptors in the central nervous system. *J Pharmacol Exp Ther* **299**:12-20.
- Schoepp DD, Jane DE and Monn JA (1999) Pharmacological agents acting at subtypes of metabotropic glutamate receptors. *Neuropharmacology* **38**:1431-176.
- Seifert R, Wenzel-Seifert K, Gether U and Kobilka BK (2001) Functional differences between full and partial agonists: evidence for ligand-specific receptor conformations. *J Pharmacol Exp Ther* **297**:1218-1226.
- Thomas NK, Wright RA, Howson PA, Kingston AE, Schoepp DD and Jane DE (2001) (S)-3,4-DCPG, a potent and selective mGlu8a receptor agonist, activates metabotropic glutamate receptors on primary afferent terminals in the neonatal rat spinal cord. *Neuropharmacology* **40**:311-318.
- Thompson JD, Higgins DG and Gibson TJ (1994) CLUSTAL W: improving the sensitivity of progressive multiple sequence alignment through sequence weighting, position-specific gap penalties and weight matrix choice. *Nucleic Acids Res* **22**:4673-4680.
- Triballeau N, Acher F, Brabet I, Pin JP and Bertrand HO (2005) Virtual screening workflow development guided by the "receiver operating characteristic" curve approach. Application to high-throughput docking on metabotropic glutamate receptor subtype 4. *J Med Chem* **48**:2534-2547.
- Tsuchiya D, Kunishima N, Kamiya N, Jingami H and Morikawa K (2002) Structural views of the ligand-binding cores of a metabotropic glutamate receptor complexed with an antagonist and both glutamate and Gd³⁺. *Proc Natl Acad Sci U S A* **99**:2660-2665.
- Venkatachalam CM, Jiang X, Oldfield T and Waldman M (2003) LigandFit: a novel method for the shape-directed rapid docking of ligands to protein active sites. *J Mol Graph Model* **21**:289-307.
- Wilson J, Brown D, Arora J, Kang J, Grabell J, Heaton W, Isaac M, Jacobson P, Johnson E, Joseph B, Kril Y, Levinthal C, Liu JW, Pierson E, Simpson T, Powel R, Ray R, Slassi A, Storjohann L, Stormann T, Trivedi S, Urbanek R, Wilkins D, Bostwick R, Hartman D and Chhajlani V (2005) Identification of novel positive allosteric modulators of mGlu8 receptor. *Neuropharmacology* **49 (Suppl.)**:278-278.

Footnotes

§: This work was supported by a grant from the ANRT (CIFRE n°403/2003) to MF, from European Community (6° PCRDT: STREP LS HB-CT 2003- 503337) for JPP and LP, and the Comité Parkinson Fondation de France (N°: 580062), and the French Government Ministry of Research (ANR-05-NEUR-0121-04) for FA, NT, JJP and LP.

Legends to figures

Figure 1. Comparative effects of FP0429 on wt mGlu4 and mGlu8 receptors. (A). Structure of group III mGlu specific agonist FP0429. This compound belongs to the recently described family of amino-pyrrolidine tricarboxylic acids (APTCS), that are products from medicinal chemistry around the group III mGlu agonist ACPT-I. (B,C). Dose-response curves of Glu and FP0429 on rat wt mGlu4 (B) or mGlu8 (C). HEK 293 cells were electroporated with plasmids encoding rat wt mGlu receptor and a chimeric G protein, allowing receptor coupling to the Phospholipase C (PLC) pathway. Transfected cells were loaded with 1 μ M Fluo4-AM, and then monitored for intracellular Ca²⁺ mobilization upon agonist addition using FlexStation II (Molecular Devices). Data are from one experiment representative of at least three independent experiments performed in triplicates, and used to determine mean EC50s (Table 1).

Figure 2. FP0429 is a partial agonist of wt mGlu8 receptor. (A,B). Comparison of the functional responses mediated by Glu, ACPT-I and FP0429 to assess full/partial agonist activity on subtypes mGlu4 (A) and 8 (B). Cells were transfected with increasing amounts of wt mGlu4 (A) or mGlu8 (B) plasmid DNA (encoding HA-tagged receptors), and were then assayed for intracellular Ca²⁺ mobilization with maximal doses of Glu (100 μ M), ACPT-I (100 μ M) or FP0429 (1mM). For each transfection, the corresponding expression level of cell surface receptor was quantified by anti-HA ELISA assay. (C). Bivalent agonist and antagonist activity of FP0429 regarding wt mGlu8. mGlu8-transfected cells were challenged with FP0429 either alone or in combination with a sub-maximal Glu dose (5 μ M). The K_B value was determined using the equation $K_B = IC_{50} / (1 + L / EC_{50})$ where L is the Glu concentration used in the experiment (5 μ M) and EC50 the mean Glu EC50 on wt mGlu8 (1.3 μ M; see Table

1). Data are from one experiment representative of at least three independent experiments performed in triplicates.

Figure 3. Identification of the LBD residues potentially involved in FP0429 partial agonist activity at mGlu8. (A). Residues involved in binding of ACPT-I in mGlu4 LBD. ACPT-I was docked in the 3D homology model of wt mGlu4 (Bertrand et al., 2002), which is based on mGlu1 VFT crystal structure (1ewk:A). The resulting ionic and H-bond network (black dashed lines) is represented in a 2D scheme, revealing that 15 residues are involved in direct ACPT-I binding or closely surrounding it. (B). Multiple sequence alignments of wt mGlu4 and mGlu8. Rat, mouse and human sequences were aligned using the ClustalW algorithm (InfoBiogen). Out of the 15 residues directly involved in ACPT-I binding or surrounding it, only 2 (framed) are not conserved between mGlu4 and mGlu8, and were submitted to site-directed mutagenesis.

Figure 4. Expression and function of mGlu4 and mGlu8 mutant receptors. (A,C). HEK 293 cells were transiently transfected with plasmids encoding HA-tagged versions of the various mutants constructed for mGlu4 (A) (mGlu4SA, mGlu4AG, mGlu4AA) or mGlu8 (C) (mGlu8SA, mGlu8AG, mGlu8SG). Mutant receptor expression was evaluated against their wt counterparts by anti-HA ELISA assay, on either non-permeabilized cells (NP) (to estimate cell surface expression) or Triton-permeabilized cells (P) (to determine total expression). (B,D). Cells transiently transfected with either mGlu4 (B) or mGlu8 (D) mutants were assayed for Ca²⁺ mobilization upon addition of a maximal Glu dose (100μM) to assess mutant functionality in comparison with wt receptors. Data are from one experiment representative of at least three independent experiments performed in triplicates.

Figure 5. Impact of the mutations on FP0429 agonist activity. (A,B). Dose-response curves of Glu and FP0429 on wt and mutant mGlu4 (A) and mGlu8 (B) receptors. (C). Comparison of the functional responses mediated by Glu, ACPT-I and FP0429 to assess full/partial agonist activity on mutant receptor mGlu8SG (“mGlu4-like”). Cells were transfected with increasing amounts of plasmid DNA encoding HA-tagged mGlu8SG receptor, and were then monitored for intracellular Ca^{2+} signals upon application of Glu (100 μM), ACPT-I (100 μM) or FP0429 (1mM). For each DNA quantity, the corresponding expression level of cell surface receptor was quantified by anti-HA ELISA assay. Represented data are either averaged data (A) or data from one representative experiment (B, C) of at least three independent experiments performed in triplicates, and used to determine mean EC50s (Table 1).

Figure 6. FP0429 docking in 3D models of mGlu4 and mGlu8 LBD. (A,B). Residues involved in binding of FP0429 in mGlu4 (A) and mGlu8 (B) LBD 3D models. FP0429 was docked in the mGlu4 and mGlu8 3D homology models, which are based on mGlu1 VFT crystal structure (1ewk:A). The resulting ionic and H-bond networks (black dashed lines) are represented in a 2D scheme, revealing that the residues involved in direct ligand binding or closely surrounding it, slightly vary between wt mGlu4 and mGlu8, possibly explaining the differential agonist activity regarding those two subtypes. Residues from lobe I are colored in cyan, those of lobe II in magenta and hinge in orange. (C, D). Snapshots of FP0429 docked in wt mGlu4 and mGlu8 LBD 3D models. Only distal residues binding FP429 are displayed. Colour code for protein residues same as Figure 6A and B, for FP429 atoms: carbon grey, oxygen red, nitrogen blue. Polar interactions (hydrogen bonds and ionic interactions) are shown as green dashed lines. (E). Snapshots of FP0429 docked in wt mGlu4 (grey) or mGlu8 (pink) LBD 3D superimposed models. Residues S157/G158 (mGlu4) and A154/A155 (mGlu8) are represented with their side chains. A shift (arrow) in FP0429 positioning can be

observed in the presence of the methyl groups of the 2 Ala residues (mGlu8). Models were superimposed based on the backbone of the residues of the signature motif.

Tables

Table 1. Mean Glu or FP0429 EC50s and FP0429 Emax values (%Glu max) for wt and mutant mGlu4 and mGlu8 receptors. All dose-response curves were fitted using GraphPad Prism 4. At least three independent experiments performed in triplicates were used to determine mean EC50s and Emax values.

| Receptor | mGlu4wt | mGlu4SA | mGlu4AG | mGlu4AA | mGlu8wt | mGlu8SA | mGlu8AG | mGlu8SG |
|-----------------------------------------------|----------------|----------------|----------------|-----------------|-----------------|----------------|-----------------|----------------|
| Glu EC50 (μM) | 3.0 \pm 0.3 | 3.8 \pm 0.3 | 3.2 \pm 0.4 | 2.8 \pm 0.5 | 1.3 \pm 0.5 | 0.8 \pm 0.1 | 0.9 \pm 0.1 | 1.1 \pm 0.2 |
| FP0429 EC50 (μM) | 48.3 \pm 5.2 | 40.1 \pm 3.8 | 48.9 \pm 8.3 | 79.6 \pm 14.3 | 56.2 \pm 14.6 | 47.3 \pm 5.1 | 71.2 \pm 14.2 | 50.8 \pm 5.7 |
| FP0429 Emax (%Glu max) | 75 \pm 6 | 45 \pm 4 | 76 \pm 4 | 52 \pm 9 | 36 \pm 7 | 52 \pm 8 | 70 \pm 11 | 90 \pm 16 |

Figure 1

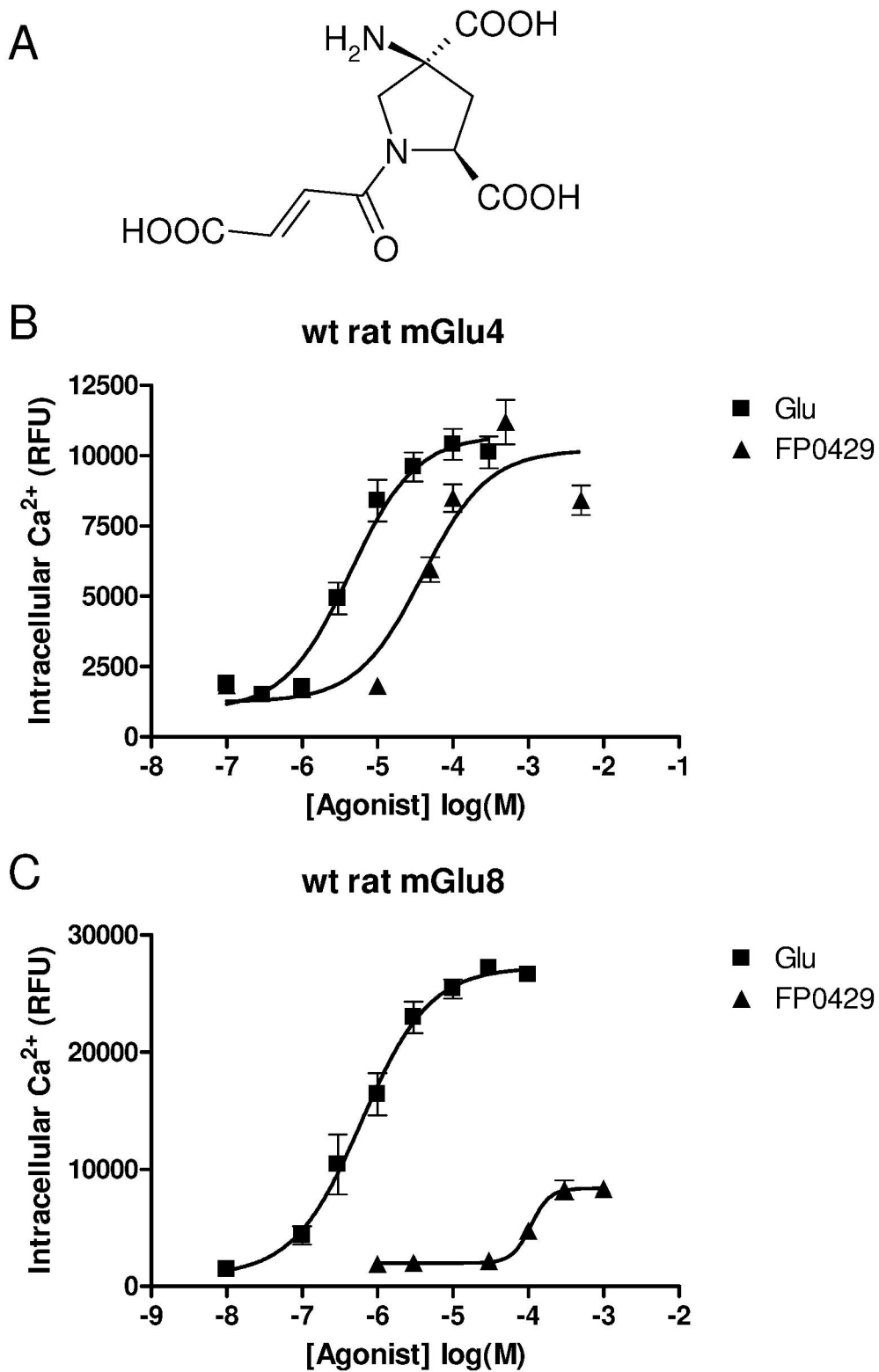


Figure 2

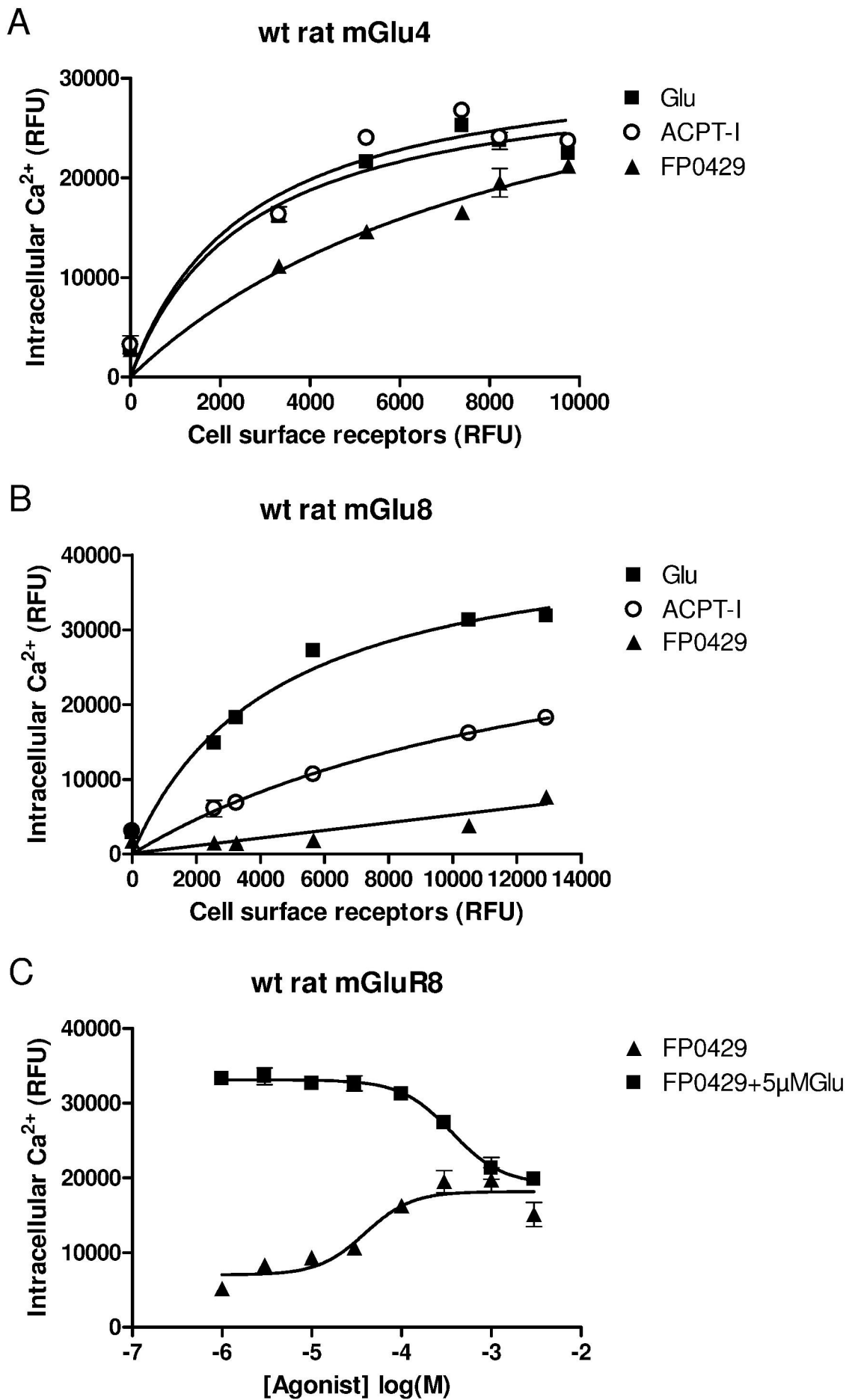
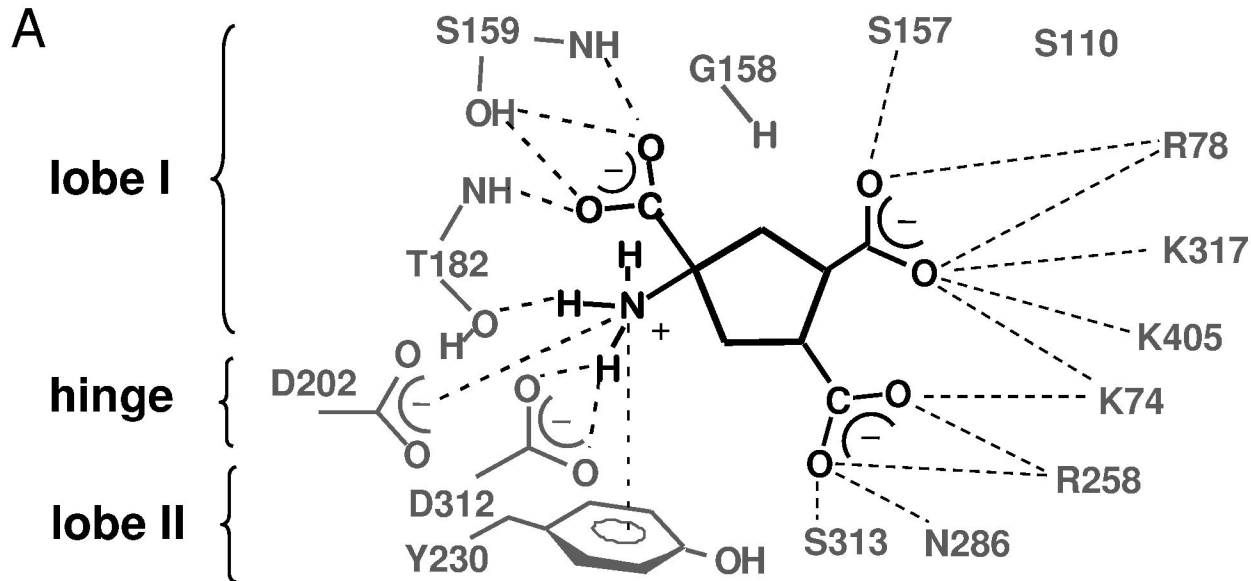


Figure 3



B

| | | | | | | | | | | |
|-------------|-----------|----|------|-----|---------|-----|-------|-----|-------|-----|
| Rat mGlu8 | KEKGIHRLE | 77 | TCSR | 109 | GAAASSV | 158 | ASTAP | 181 | PPDSY | 201 |
| Human mGlu8 | KEKGIHRLE | 77 | TCSR | 109 | GAAASSV | 158 | ASTAP | 181 | PPDSY | 201 |
| Mouse mGlu8 | KEKGIHRLE | 77 | TCSR | 109 | GAAASSV | 158 | ASTAP | 181 | PPDSY | 201 |
| Rat mGlu4 | KEKGIHRLE | 80 | TCSR | 112 | GASGSSV | 161 | ASTAP | 184 | PSDTY | 204 |
| Human mGlu4 | KEKGIHRLE | 80 | TCSR | 112 | GASGSSV | 161 | ASTAP | 184 | PSDTY | 204 |
| Mouse mGlu4 | KEKGIHRLE | 80 | TCSR | 112 | GASGSSV | 161 | ASTAP | 184 | PSDTY | 204 |

| | | | | | | | | | | |
|-------------|-------|-----|-------|-----|-------|-----|------------|-----|-------|-----|
| Rat mGlu8 | GNYGE | 229 | IPREP | 257 | FANED | 285 | GSDSWGSKIA | 316 | EGKVQ | 403 |
| Human mGlu8 | GNYGE | 229 | IPREP | 257 | FANED | 285 | GSDSWGSKIA | 316 | EGKVQ | 403 |
| Mouse mGlu8 | GNYGE | 229 | IPREP | 257 | FANED | 285 | GSDSWGSKIA | 316 | EGKVQ | 403 |
| Rat mGlu4 | GSYGE | 232 | IPREP | 260 | FANED | 288 | GSDSWGSKIA | 319 | EGKVQ | 407 |
| Human mGlu4 | GSYGE | 232 | IPREP | 260 | FANED | 288 | GSDSWGSKIA | 319 | EGKVQ | 407 |
| Mouse mGlu4 | GSYGE | 232 | IPREP | 260 | FANED | 288 | GSDSWGSKSA | 319 | EGKVQ | 407 |

Figure 4

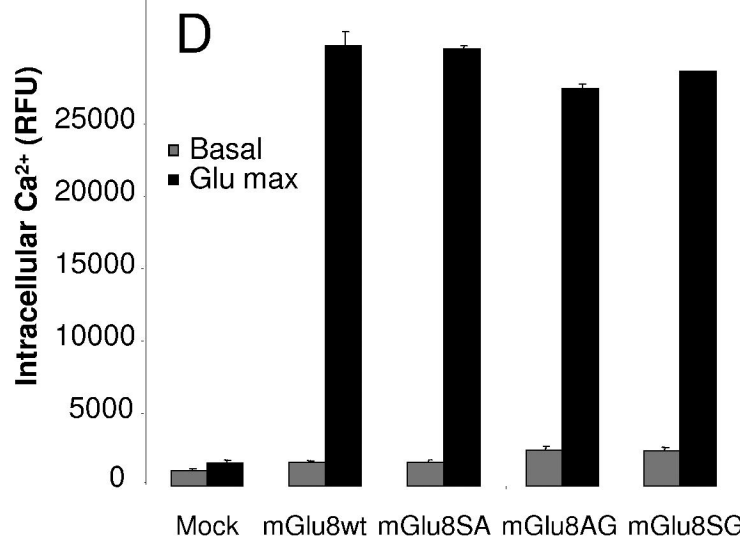
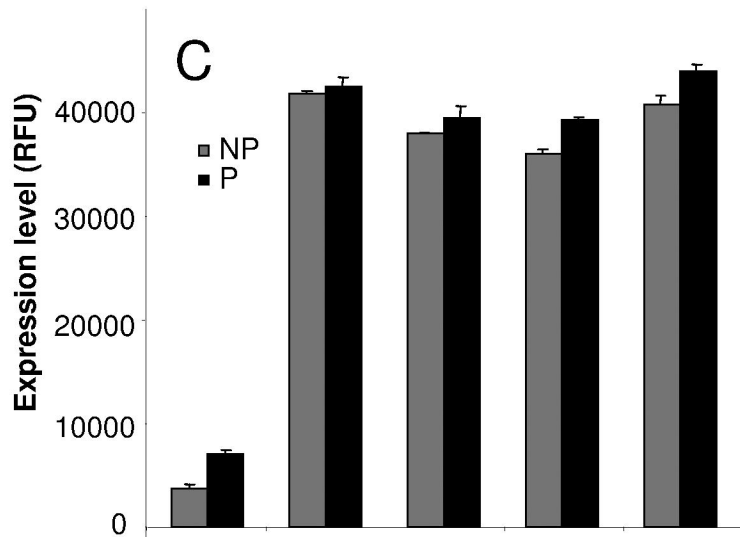
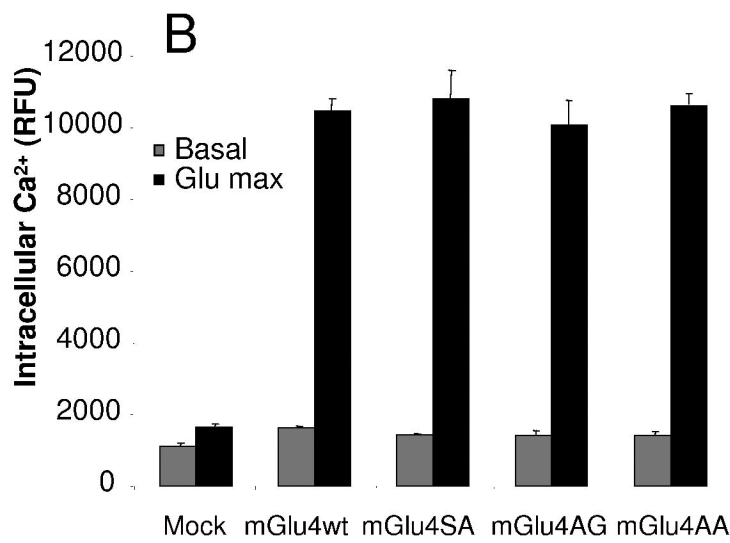
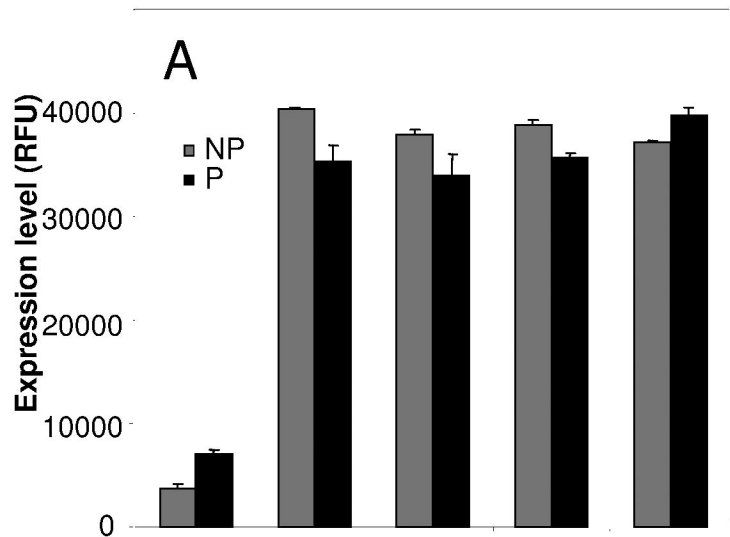


Figure 5

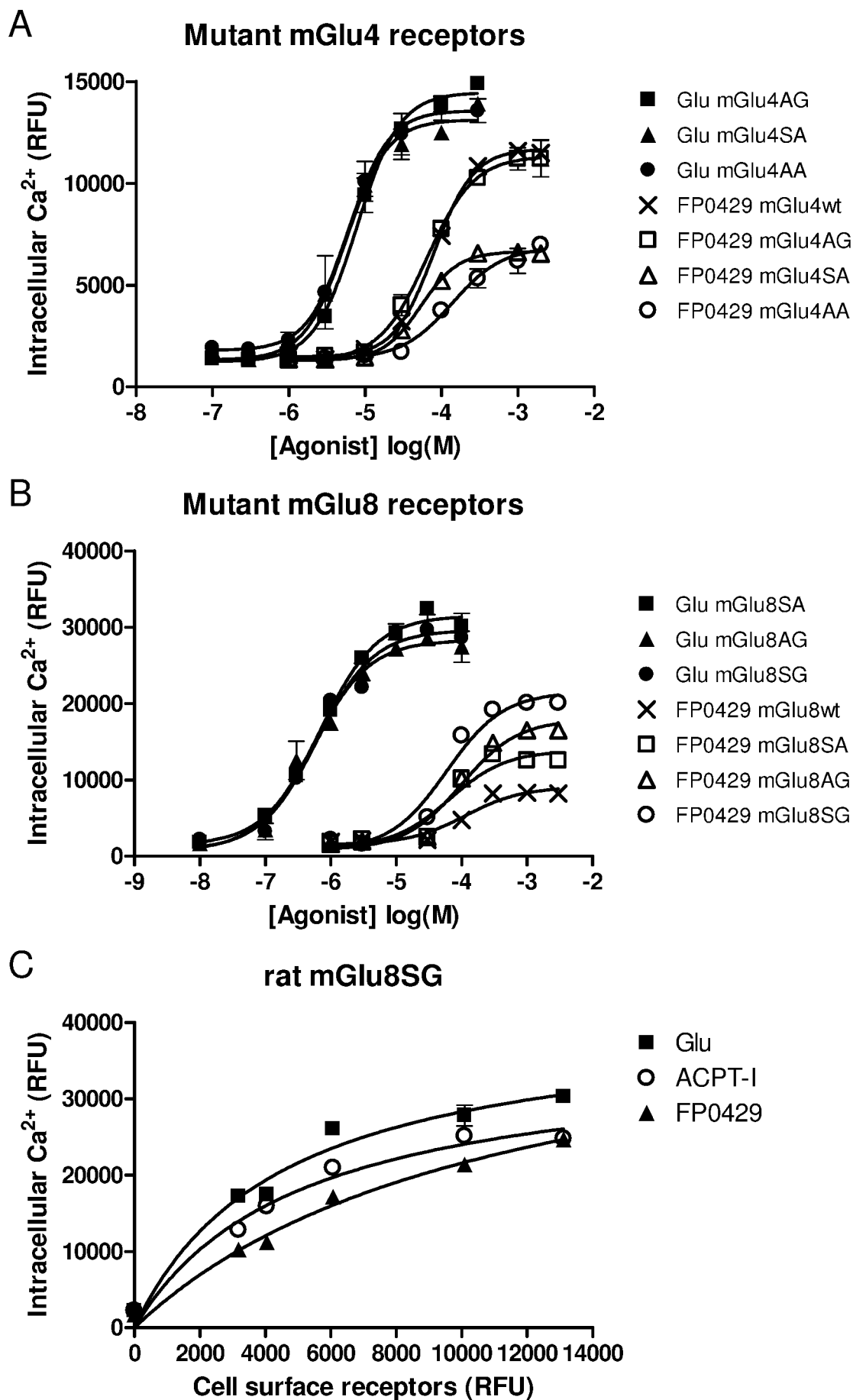
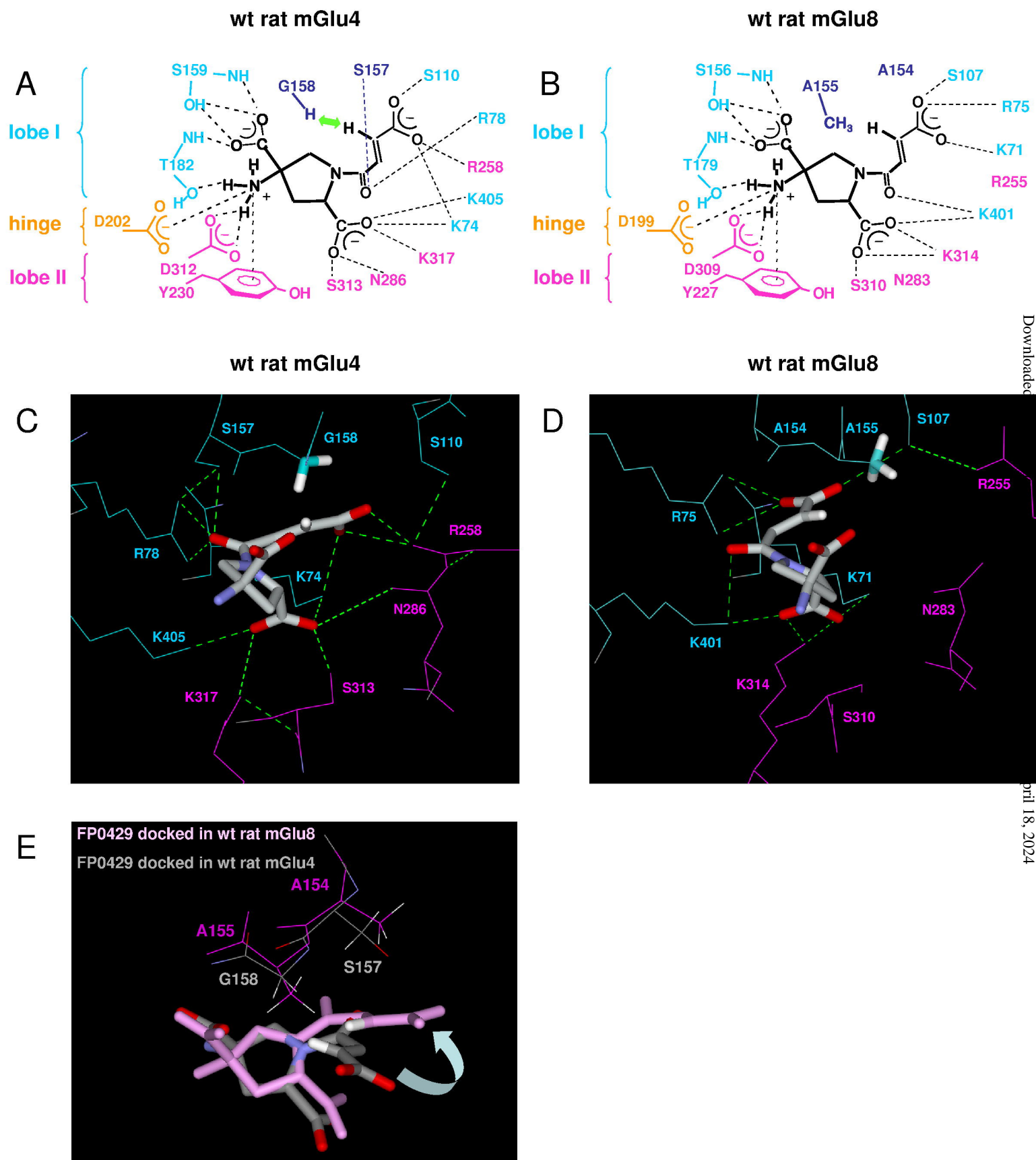


Figure 6



Downloaded

April 18, 2024